Available online at www.sciencedirect.com
ScienceDirect
European Polymer Journal 44 (2008) 968–977
EUROPEAN POLYMER JOURNAL
www.elsevier.com/locate/europolj

Macromolecular Nanotechnology

Physical and tribological properties of a new polycarbonate-organoclay nanocomposite

Francisco J. Carrión [a,*], Alejandro Arribas [b], María-Dolores Bermúdez [a], Antonio Guillamon [c]

[a] *Grupo de Ciencia de Materiales e Ingeniería Metalúrgica, Departamento de Ingeniería de Materiales y Fabricación, Universidad Politécnica de Cartagena, Campus de la Muralla del Mar, C/Doctor Fleming s/n, 30202 Cartagena, Spain*
[b] *Centro Tecnológico del Calzado y Plástico de la Región de Murcia, Polígono Industrial Las Salinas, Avda, Europa, 4–5, 30840 Alhama de Murcia, Spain*
[c] *Grupo de Modelos y Sistemas, Departamento de Matemática Aplicada y Estadística, Universidad Politécnica de Cartagena, Campus de la Muralla del Mar, C/Doctor Fleming s/n, 30202 Cartagena, Spain*

Received 22 October 2007; received in revised form 18 January 2008; accepted 31 January 2008
Available online 9 February 2008

Abstract

A new polycarbonate (LS2) nanocomposite containing a 3 wt% proportion of the organically modified montmorillonite bentone 2010 (B 2010) has been prepared by extrusion and injection moulding, and its tribological properties determined under a pin-on-disc configuration against stainless steel. The nanocomposite (LS2 + 3% B 2010) presents a 88% reduction in friction and up to two orders of magnitude reduction in wear rate with respect to the base polymer. The new nanocomposite has been characterized by transmission electron microscopy (TEM) and X-ray diffraction (XRD), and its thermal and dynamic mechanical properties have been determined by differential scanning calorimetry (DSC), thermogravimetric analysis (TGA) and dynamic mechanical analysis (DMA) techniques. The nanocomposite shows a uniform dispersion of the nanoclay as pointed out by two different statistical methods. The good tribological performance of the new nanocomposite is attributed to this uniform microstructure and to the increase in the nanoclay stacking distance.

Keywords: Polycarbonate; Organo-modified montmorillonite; Nanocomposite; Friction; Wear

1. Introduction

There exists a great interest in the development of new polymer-clay nanocomposites in the expectation of improved physicochemical and mechanical properties with respect to the pure polymers and conventional composites, with the use of a relatively low filler proportion [1].

Polymer nanocomposites based on layered silicates (e.g., montmorillonite, MMT) have been widely investigated [2–9]. The montmorillonites are layered silicates which consist of stacked platelets with a thickness of the order of 1 nm. Montmorillonites are naturally hydrophilic and they are modified

* Corresponding author. Tel.: +34 968325959; fax: +34 968326445.
E-mail address: fjc.vilches@upct.es (F.J. Carrión).

0014-3057/$ - see front matter © 2008 Elsevier Ltd. All rights reserved.
doi:10.1016/j.eurpolymj.2008.01.038

by ion exchange, e.g., with quaternary ammonium salts, in order to increase their organophilic characteristics. These modified clays, also called organoclays present better compatibility with polymer matrices [10]. Melt intercalation is a method to obtain nanocomposites, and the intercalation is improved by the use of conventional processing [11]. Extrusion has proved to be effective in the exfoliation and dispersion of the layered silicate.

Polycarbonate is an amorphous engineering thermoplastic which combines good thermal stability, transparency, impact resistance and the ability to be processed on conventional machinery. Thus, the surface properties are important for many applications such as medical, optics, automobile, etc., since problems related to scratching or wear on the surface are of interest in the case of this thermoplastic.

New polycarbonate nanocomposites [4–6] are being developed in order to improve the thermal, mechanical, electrical or optical properties of the base polymer.

Recent works have developed new clay-reinforced polycarbonate nanocomposites using microwave-aided solid state polymerization [4] or blending with a miscible polymer which contains the dispersed nanoclay [5].

Due to the relatively low degradation temperatures of the organic modifiers, there has been only one previous attempt to develop polycarbonate nanocomposites based on melt intercalation of layered silicates [12].

Previous studies on wear behaviour of clay nanocomposites are rather limited [13–21], and no tribological properties of polycarbonate-clay nanocomposites have been described so far.

We have recently described the tribological performance of new polycarbonate nanocomposites containing ZnO nanoparticles [22], and their wear resistance improvement by nanoparticles modification with imidazolium ionic liquids [23].

In the present paper we describe the preparation, characterization and tribological properties of a new polycarbonate-organoclay nanocomposite.

2. Experimental section

The starting polycarbonate material was Lexan LS2 from General Electric Plastics. The quaternary ammonium-modified montmorillonite Bentone 2010® was supplied by Elementis Specialties and used as received.

Polycarbonate (LS2) was blended with a 3 wt% of Bentone 2010 (B 2010) at 220 °C using a twin screw co-rotating extruder Leistritz ZSE 18HP 40 D, with a screw speed of 100 rpm. The extruded blend was injection moulded at 210 °C in a DEU 250H55 mini VP injection machine with a mould temperature of 80 °C, to obtain the nanocomposite (LS2 + 3% B 2010). The same procedure was followed for neat polycarbonate.

XRD patterns were recorded using a Bruker D8 Advance XRD diffractometer equipped with a Göbel mirror, using Cu Kα radiation of 1.54 Å with a voltage of 40 kV and 40 mA of current intensity.

Differential scanning calorimetry (DSC) studies were performed using a Mettler Toledo DSC 822. Samples of 7.855 mg for LS2 and 7.255 mg for LS2 + 3% B 2010 were heated above the T_g, then remained at 300 °C for 5 min, quenched, and measured on the second heating between 0 and 300 °C, at a heating rate of 20 °C/min in nitrogen atmosphere, with a flow rate of 50 ml/min.

Thermogravimetric analysis (TGA) was carried out using a Mettler Toledo TGA SDTA 851 analyzer at a heating rate of 20 °C/min from 30 °C to 950 °C in oxygen flow of 40 ml/min.

Dynamic mechanical analysis (DMA) was carried out with a TA Q800 DMA equipment under the single cantilever mode at an oscillatory frequency of 1 Hz, under a 1% strain, for a temperature range from −130 °C to 170 °C at a heating rate of 3 °C/min.

Hardness values of the polymers were determined with a Shore D hardness tester TH210.

Pin-on-disc tests according to ASTM G 99-05 standard were performed as previously described [22,23] on 40 mm diameter, 4 mm height polymer discs sliding against AISI 316 L (composition: <0.03% C; 17.55% Cr; 13% Ni; 2.5% Mo; hardness: 210 HV) stainless steel pins with 0.8 mm spherical end radius. Experimental tribological parameters were: wear track radius = 9 mm; sliding speed = 0.10 m s^{-1}; and sliding distance = 500 m. Normal load was 0.98 N with a mean contact pressure of 74.6 MPa. Polymer discs roughness (R_a) before the tests was 0.5–0.8 μm. Friction coefficients were continuously recorded with time for each test and wear rates were calculated from wear track width measurements.

Optical micrographs were obtained using a Leica DMRX microscope. SEM images were obtained using a Hitachi S3500 N scanning electron microscope. The samples were sputter coated with a thin

layer of gold in order to make them conductive with the aid of a SC7640 Sputter Coater of Polaron Division.

A Jeol JEM-2010 transmission electron microscope was used to characterize the structure of the blend.

3. Results and discussion

3.1. Material characterization and microstructure

The TEM micrograph of a thin slice of LS2 + 3% bentone in Fig. 1 shows the homogeneous distribution and the preferential orientation of the nanoclay phase into the polycarbonate matrix that occurs during the injection moulding process. Fig. 2 compares the microstructure of the neat nanoclay (Fig. 2A), where the layered silicate particles are randomly oriented, with that of the nanoclay embedded in the polymer matrix (Fig. 2B), which shows a parallel orientation.

A slight increase in hardness (Table 1) is obtained by the addition of the nanoclay. This result, together with the good dispersion (see Section 3.2) and the intercalation commented above, anticipated a good tribological performance of the new nanocomposite.

The X-ray diffraction pattern (Fig. 3) of the starting nanoclay Bentone 2010 shows a peak at $2\theta = 4.5°$, corresponding to a d-spacing of 2.00 nm. This peak is not present in the nanocomposite LS2 + 3% B 2010 diffractogram, which presents two peaks. The main peak at $2\theta = 2.9°$ corresponds to a stacking distance of 3.06 nm. This higher distance indicates that the intercalation of the polymer between the silicate layers has taken place. A minor peak in the diffractogram of the nanocomposite is observed at a higher angle of 5.8°, which corresponds to a distance of 1.53 nm, one half of the stacking distance of 3.06 nm, and therefore can be assigned to a second order diffraction [5].

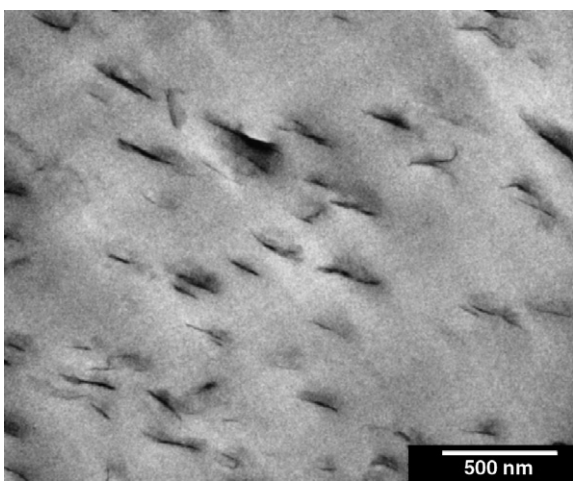

Fig. 1. TEM micrograph of LS2 + 3% B 2010 showing the distribution of the nanoclay dispersed phase.

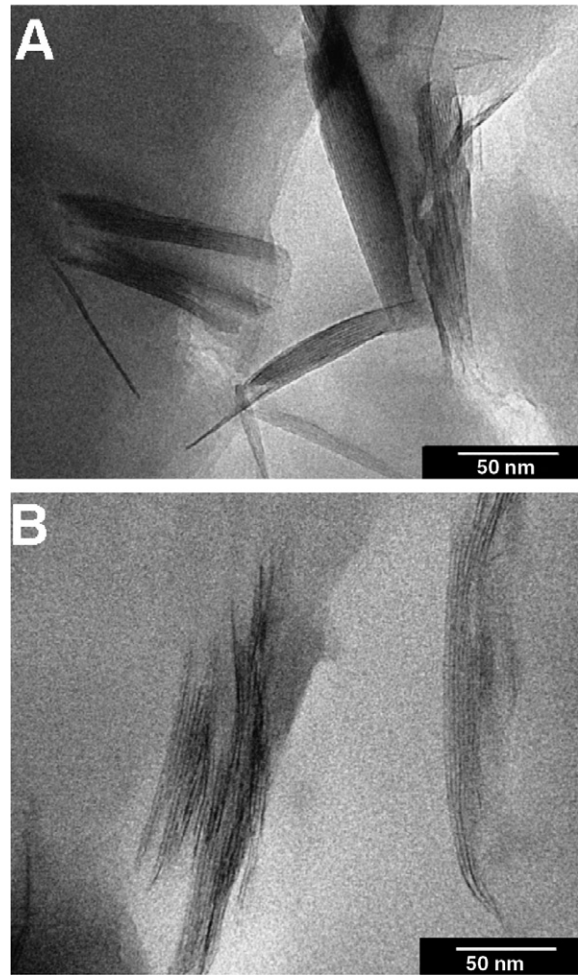

Fig. 2. TEM micrographs of: (A) Starting nanoclay; (B) Nanoclay particles embedded in the polycarbonate matrix.

Table 1
Hardness values (standard deviation)

Material	LS2	LS2 + 3% B 2010
Hardness Shore D	81.3 (0.082)	83.6 (0.35)

3.2. Spatial distribution of nanoclay particles

It is well known that the mechanical properties of particulate composite materials depend not only on

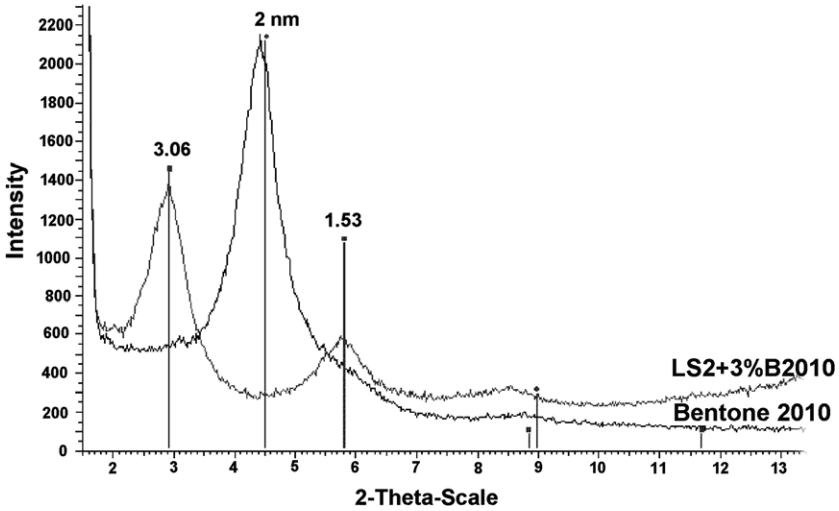

Fig. 3. XRD patterns for neat nanoclay (Bentone 2010) and for polycarbonate nanocomposite (LS2 + 3% B 2010).

the shape and the volume fraction, but also on the spatial distribution of the reinforcing particles held in the matrix [24,25].

In order to check the uniformity of the distribution of the nanoclay particles a statistical study of spatial distribution has been developed using the *quadrat method* [25] and the *nearest-neighbour method* [26,27].

Fig. 4A shows a low magnification TEM micrograph of the nanoclay distribution within the PC matrix. If the analyzed surface (Fig. 4A) is divided into m rectangular cells of equal size (Fig. 4B), n_i denotes the observed value of points in ith cells, and n is the total number of points, the Morisita's index is defined by:

$$I_m = m\frac{\sum_{i=1}^{m} n_i(n_i-1)}{n(n-1)} \quad (1)$$

Then, when points present a random and homogeneous spatial distribution, I_m is independent of the cells size and fluctuates around 1 (the mean value), whereas if clusters are presented, I_m becomes greater than 1.

If one simply looks at distances between points and their nearest neighbours, then this provides a natural statistical test that requires no artificial partitioning scheme. More precisely, if d_i denotes the *nearest neighbour euclidean distance* (*nn-distance*) from the ith points to the rest of all other points, the average magnitudes of these nn-distances provide a direct measure of "uniformity" or "clustering" for points patterns.

In a uniform spatial dispersion pattern the nearest neighbour distances will be large, whereas in a clumped pattern they should be small. If we denote by d_i the *nn-distance* from the ith point *to* the other, n the total number of points and λ the points density, the mean of the observed nearest neighbour distances (d_0) and the expected mean of the nearest neighbour distances (d_E), for a random dispersion pattern are given by $d_0 = \frac{1}{n}\sum_{i=1}^{n} d_i$, and $d_E = \frac{1}{2\sqrt{\lambda}}$, respectively.

In the Clark–Evans method, the mean of the observed nearest neighbour distances is compared to the following dispersion index (D):

$$D = \frac{d_0}{d_E} \quad (2)$$

Then, if the spatial distribution of points is homogeneous, D fluctuates around the mean value of 1, whereas if clusters are presented, D becomes greater than 1.

Table 2 shows the values obtained for the different statistics. All of them guarantee the uniformity of the distribution of the particles, at least for the examined surface.

The plots in Fig. 4C and D compare the histograms of the frequencies distribution of nearest neighbour distances for the nanocomposite (Fig. 4C) with the distribution resulting from running a hundred simulations, using the MATLAB software command line (Fig. 4D).

3.3. Thermal properties

DSC thermograms in Fig. 5 shows that while neat LS2 has a glass transition temperature (T_g) of 141 °C, the T_g of the nanocomposite can be

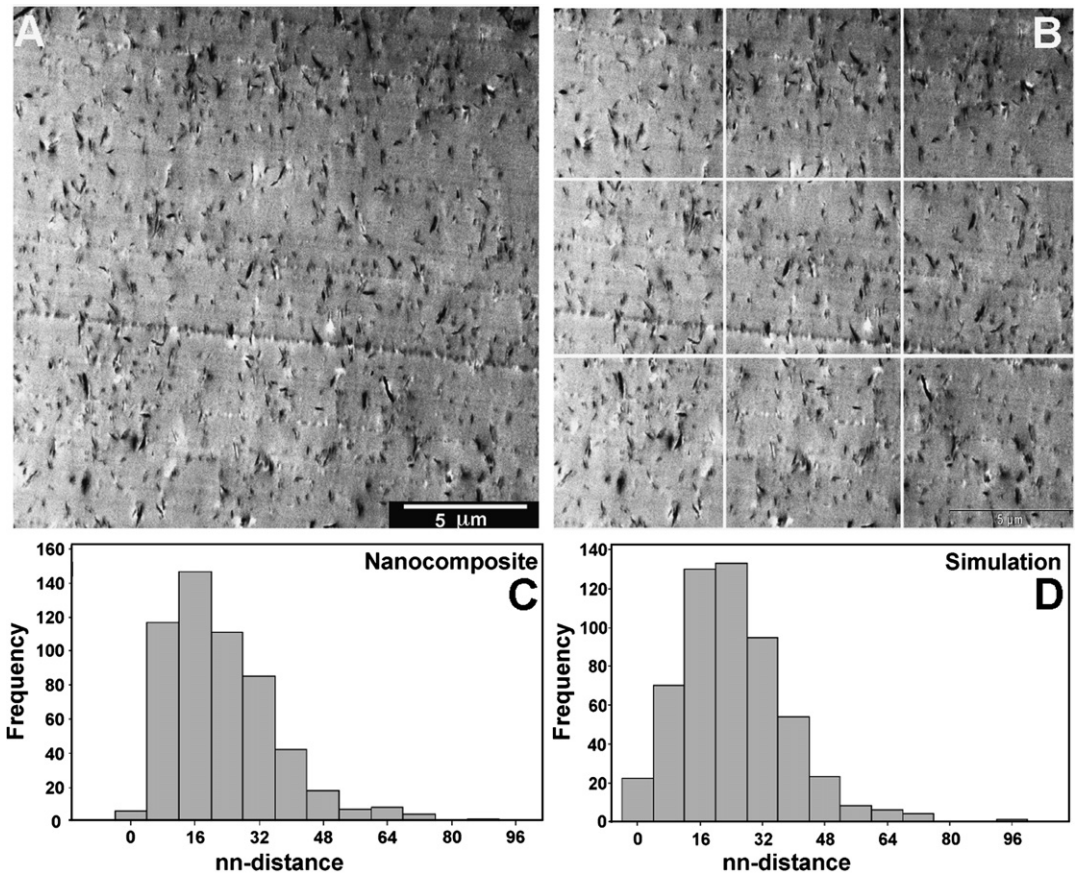

Fig. 4. (A) Original distribution of nanoclay particles; (B) Partitions of the analyzed surface according to the *Quadrat Method*; (C) Histogram of frequencies versus nearest-neighbour distances for the nanocomposite and (D) Simulation obtained using MATLAB software.

Table 2
Particle uniformity distribution statistical results

Quadrat method			
	Four cells	Nine cells	16 cells
Morisita index	$I_4 = 1.0033$	$I_9 = 1.0032$	$I_{16} = 1.0038$
Nearest-Neighbour method			
Clark–Evans test	$d_0 = 22.744$; $d_E = 23.934$		
	$D = 22.744/23.934 = 0.950$		

observed at 128 °C. This 13 °C reduction in T_g shows that the nanoclay acts as a plasticizer of polycarbonate.

Fig. 6 shows TGA curves for both materials. The corresponding degradation temperatures are shown in Table 3.

Both the neat polymer and the nanocomposite present two degradation steps. The first step would correspond to complete loss of the carbonate and isopropylidene groups with partial degradation of aromatic groups [28]. The second step, is attributed to the final degradation of aromatic carbons [28].

The presence of nanoclay increases the thermal stability of polycarbonate.The thermal degradation of polycarbonate under oxygen begins at 475 °C (T onset) in contrast with 501 °C for the nanocomposite.

Dynamic mechanical analysis (DMA) curves appear in Fig. 7. Table 4 shows the results of DMA for LS2 and for LS2 + 3% B 2010 nanocomposite.

Several methods have been described for the calculation of T_g values. According to ASTM D4065-01 standard, it should be calculated using the loss modulus E'' [29]. From these curves (Fig. 7A), the glass transition temperatures appear at 143 °C for the neat polymer and at 126 °C for the nanocomposite (Table 4). Those results are consistent with the DSC data discussed above (Fig. 5) and confirm the plasticizing effect of the addition of the nanoclay into the polycarbonate.

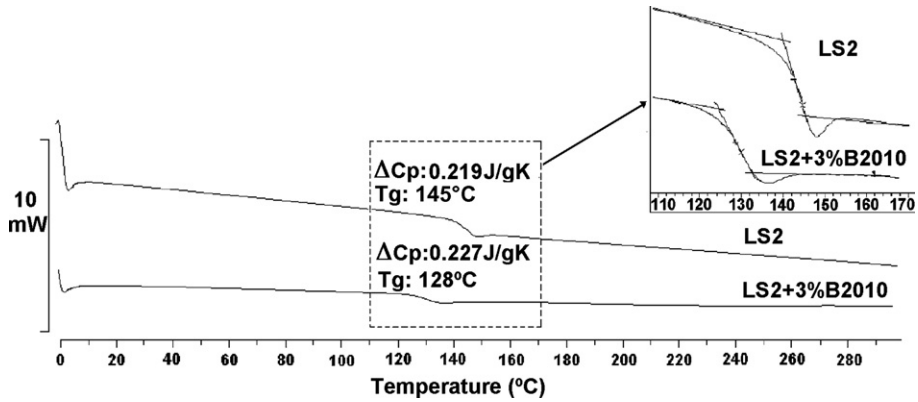

Fig. 5. DSC for neat polycarbonate (LS2) and polymer nanocomposite (LS2 + 3% B 2010).

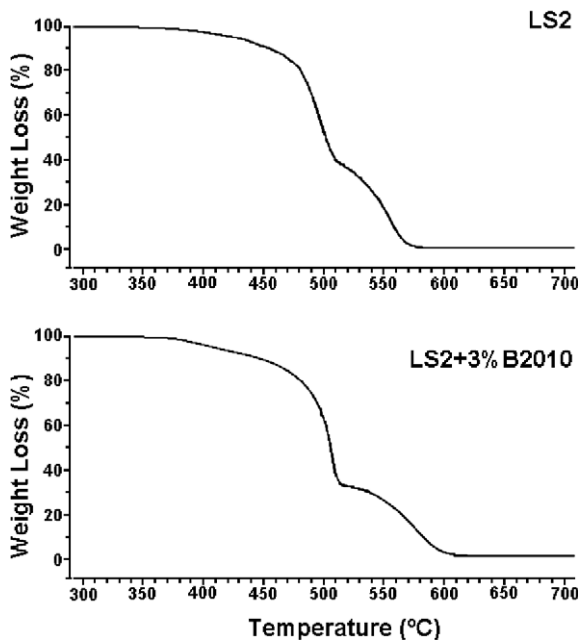

Fig. 6. TGA curves in oxygen for LS2 and LS2 + 3% B 2010 (heating rate 20 °C/min).

Table 3
Degradation temperatures for LS2 and LS2 + 3% B 2010 (heating rate of 20 °C/min in oxygen flow of 40 ml/min.)

	1st step		2nd step	
	T onset (°C)	*T* midpoint (°C)	*T* onset (°C)	*T* midpoint (°C)
LS2	475	504	552	565
LS2 + 3% B 2010	501	518	562	589

There is not a great difference between the modulus E' or E'' for the nanocomposite in comparison with neat polymer. A slight increase in storage modulus is observed for the nanocomposite (2380 MPa) with respect to the neat polymer (2148 MPa) at room temperature. On the other hand the incorporation of the nanoclay to the polycarbonate matrix yields similar values of the loss factor ($\tan\delta$). The reason could be the low quantity of nanoclay used.

3.4. Tribological properties

Table 5 shows the tribological properties of neat polycarbonate (LS2) and those of the new nanocomposite (LS2 + 3% B 2010).

Fig. 8 shows the continuously recorded friction values with sliding distance for both the neat polymer (LS2) and the nanocomposite (LS2 + 3% B 2010). As can be seen in Fig. 8, LS2 shows a low initial friction coefficient, which suddenly increases to a very high friction value after a sliding distance of 144 m. In contrast, the new nanocomposite shows a very low constant friction value.

This friction decrease by addition of nanoclay is equivalent to a transition from dry to lubricated wear regime. In fact, as shown in Table 5, a two orders of magnitude decrease in the steady-state wear rate is observed for the nanocomposite with respect to neat polycarbonate.

It is well known that the friction mechanisms depend strongly on thermal effects between the materials in contact and in motion. The intercalated nanolayers are expected to increase the thermal stability of the polymer [30]. This fact can be confirmed when the thermal degradation temperatures of neat LS2 and the nanocomposite are compared (Table 3) where the presence of the nanoclay increases the thermal degradation temperature.

The optical micrograph of the wear path on the nanocomposite (Fig. 9) shows a smooth appearance

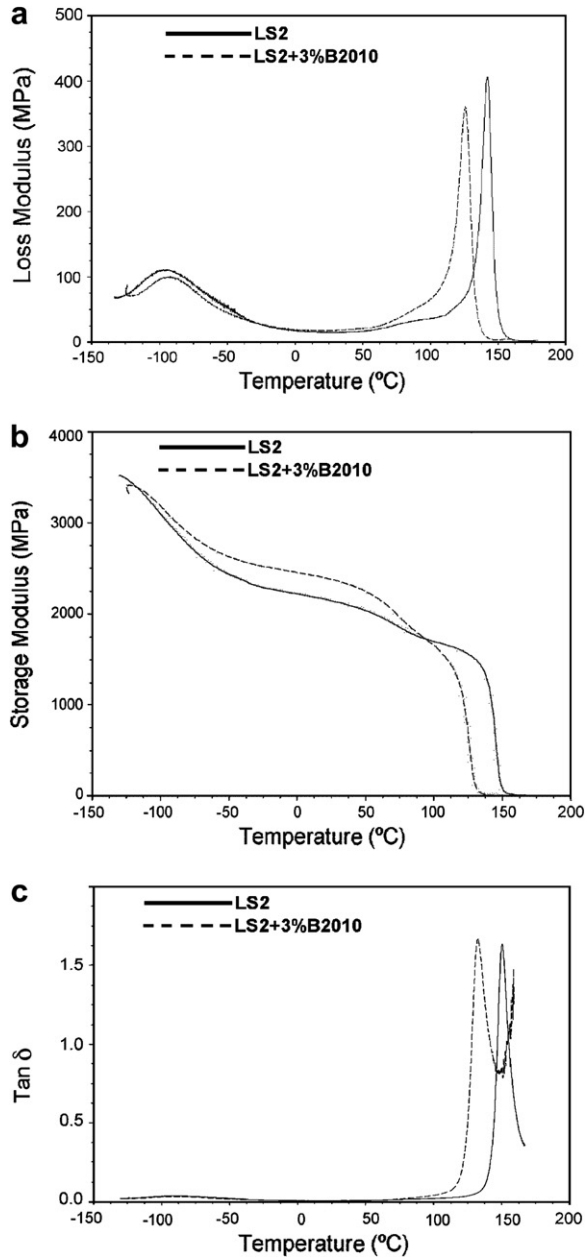

Fig. 7. Dynamic mechanical properties: (A) Loss modulus; (B) Storage modulus; (C) tan δ.

Table 4
DMA results for LS2 and LS2 + 3% B 2010 (standard deviation)

		LS2	LS2 + 3% B 2010
Storage modulus	T_β (°C)	−116	−107
	E' (MPa)	3490 (7.8)	3334 (190.9)
	T_g (°C)	140	124
	E' (MPa)	1594 (4.4)	1410 (127.9)
Loss modulus	T_β (°C)	−93	−91
	E'' (MPa)	111(0.6)	99 (5.1)
	T_g (°C)	143	126
	E'' (MPa)	398 (18.3)	360 (5.0)
tan δ	T_β (°C)	−93	−89
	E''/E'	0.04 (4×10^{-4})	0.03 (94×10^{-4})
	T_g (°C)	146	133
	E''/E'	1.52 (0.05)	1.66 (0.04)

Table 5
Friction coefficients and wear rates (standard deviation)

Tribological properties	Materials		
	LS2		LS2 + 3% B 2010
Friction coefficient	0–500 m	144–500 m	0–500 m
	0.788 (0.453)	1.091 (0.110)	0.125 (0.004)
Specific wear rate (mm^3/Nm)	1.924×10^{-3} (3.774×10^{-9})		2.854×10^{-5} (1.114×10^{-7})

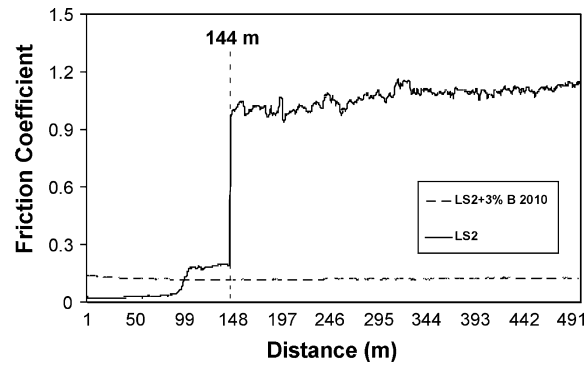

Fig. 8. Friction-sliding distance records.

(Fig. 9A). Only a mild ironing effect is observed with reduction of the surface asperities.

The high magnification SEM micrographs (Fig. 9B and C) shows signs of plastic deformation and crack initiation, corresponding to a very mild delamination wear mechanism.

In the case of neat polycarbonate (Fig. 10), a wide wear scar can be observed (Fig. 10A) corresponding to a very severe wear regime where the main wear mechanism is crack propagation which finally produces wear debris detachment (Fig. 10B and C).

Fig. 11 shows the steel pin after the test against LS2 disc. The steel pin tip surface appears covered with adhered polycarbonate particles, which have been removed from the polycarbonate disc and have remained trapped at the pin-disc contact path, thus suffering extensive plastic deformation.

However, during the initial low friction period (Fig. 6), no transference of wear debris from the

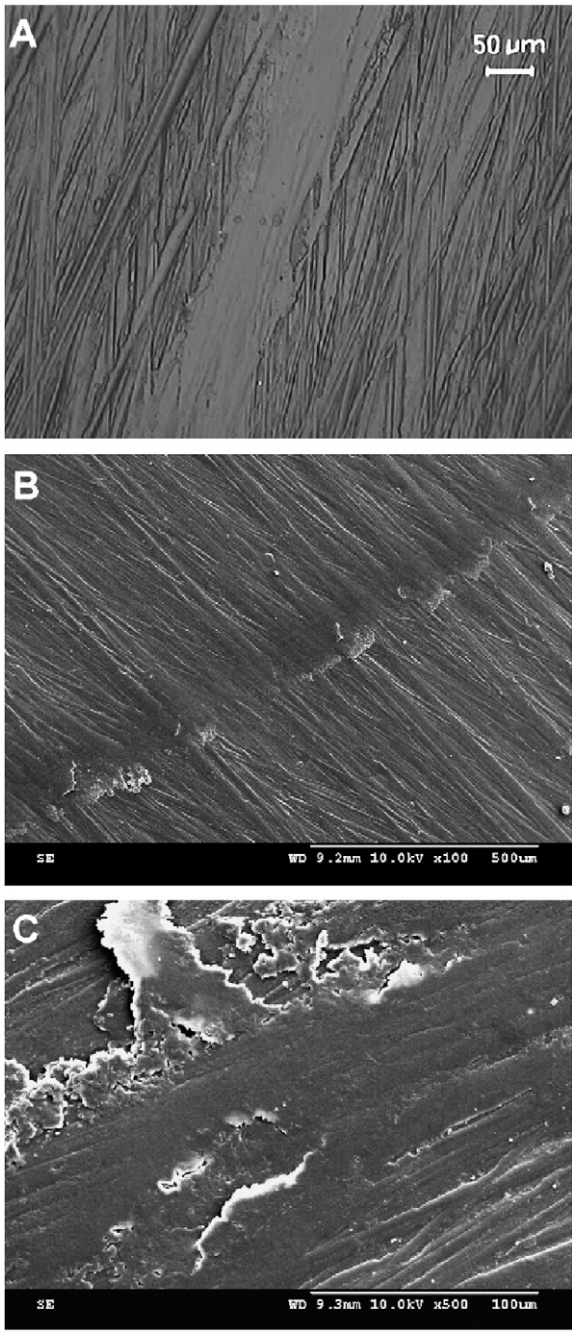

Fig. 9. (A) Optical micrograph and (B, C) SEM micrographs of the wear path on LS2 + 3% B 2010.

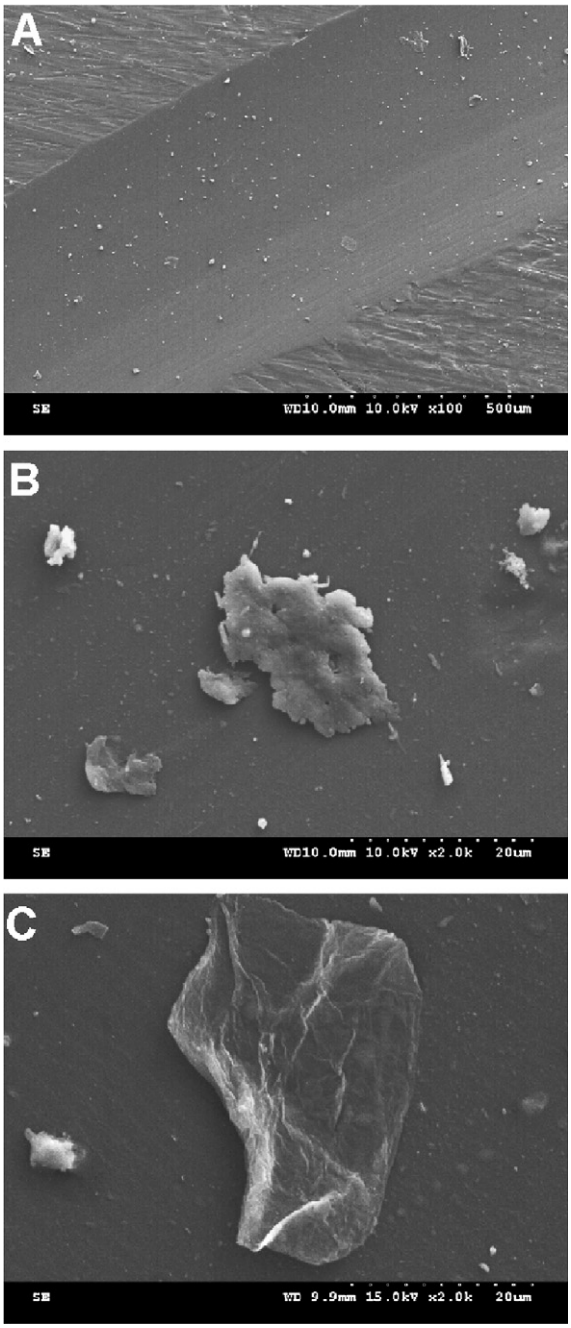

Fig. 10. SEM micrographs of: (A) Wear path on neat polycarbonate (LS2); (B and C) Wear debris.

LS2 disc to the pin is observed. Thus, the sharp friction increase could be related to the transition form break-in to steady state due to the fracture of the LS2 skin layer and massive transference of wear debris to the steel surface.

The unfilled polycarbonate is thus characterized by poor tribological performance where severe damage appears by the production of a large amount of wear particles in an adhesive-abrasive wear mechanism. Wear debris increase the abrasive wear mechanism since they operate as a third body in the

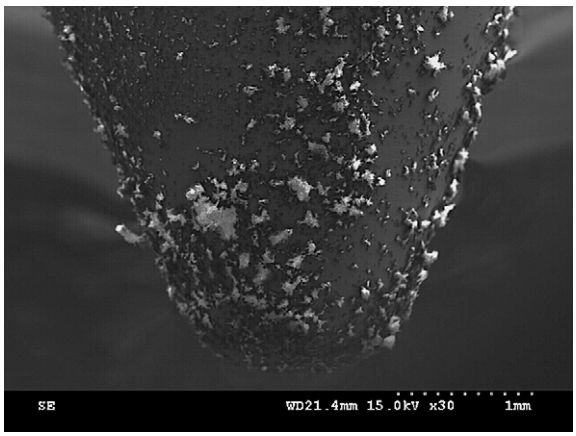

Fig. 11. SEM micrographs of the steel pin after the test against neat polycarbonate (LS2).

contact area between the steel pin and the polymer counterface.

In contrast, in the case of the nanocomposite, the steel pin surface remains free of adhered abrasive particles throughout the test. The nanoclay dispersion acts as an obstacle for the removal of polymer particles, thus preventing severe wear and maintaining the initial low friction coefficient.

The tribological behavior of a polymer-metal pair depends on the mechanical and thermal modes in the contact when the materials are in relative motion. Depending on speed, load, temperature and on the intrinsic viscoelastic properties of the polymer, the deformations and subsequent energy dissipation can occur through surface damage such as yield, plastic deformation and fracture or through the generation of heat.

In our case, the practical absence of cracks along the wear track and the smooth appearance on LS2 + % B 2010 (Fig. 9) indicates that the energy dissipation as heat prevails over the mechanical deformation and fracture mode. In contrast, LS2 (neat PC) presents severe damage (Fig. 10) with production of a large quantity of particles. This combination of thermal and mechanical effects would account for the good tribological performance of the nanocomposite.

The nanoclay platelets in the nanocomposite present a preferential orientation (Fig. 1). This orientation could have an important influence on the tribological properties of the material as a function of sliding direction. However, under the pin-on-disc configuration used in the present study, no preferential sliding direction exists, as the steel pin describes a continuous rotational motion. In order to determine the influence of nanoclay orientation, we are currently studying the scratch resistance of the nanocomposite when the sliding direction is either parallel or perpendicular to the orientation of the nanoclay.

4. Conclusions

A new polycarbonate-organomodified clay nanocomposite with a uniform distribution of the clay nanoparticles has been prepared by melt intercalation. X-ray diffraction patterns show an increase in the stacking distance of the nanocomposite as a result of the intercalation of the polymer chains between the nanoclay layers.

The thermal stability in oxygen flow is increased in the presence of the nanoclay. The new nanocomposite shows a lower glass transition temperature than that of the neat polymer. Dynamic mechanical analysis confirms the plasticizing effect of the nanoclay and the somewhat increased ease of movement of polymer chain segments in the nanocomposite.

The addition of the nanoclay particles slightly increases the hardness of neat polycarbonate. The new nanocomposite shows a friction coefficient reduction of up to 88% and a wear reduction of nearly two orders of magnitude with respect to the neat polymer. This good tribological performance is attributed to the uniform dispersion of the nanoclay, which prevents thermal degradation and removal of polymer chains.

Acknowledgements

We wish to thank the Fundación Séneca (00447-IP-04) and MEC/FEDER (MAT2005-00067) (Spain) for financial support.

References

[1] Pinnavaia TJ, Beall GW. Polymer-clay nanocomposites. New York: Wiley; 2000.
[2] Gilman JW, Awad WH, Davis RD, Shields J, Harris RH, Davis C, et al. Polymer/layered silicate nanocomposites from thermally stable trialkylimidazolium-treated montmorillonite. Chem Mater 2002;14:3776–85.
[3] Liu A, Xie T, Yang G. Comparison of polyamide-6 nanocomposites based on pristine and organic montmorillonite obtained via anionic ring-opening polymerization. Macromol Chem Phys 2006;207:1174–81.
[4] Yoo Y, Choi KY, Lee JH. Polycarbonate/montmorillonite nanocomposites prepared by microwaved-aided solid state polymerization. Macromol Chem Phys 2004;205:1863–8.

[5] González I, Eguiazábal JI, Nazábal J. New clay-reinforced nanocomposites based on a polycarbonate/polycaprolactone blend. Polym Eng Sci 2006;46(7):864–73.
[6] Hsieh AJ, Moy P, Beyer FL, Madison P, Napadensky E, Ren JX, et al. Mechanical response and rheological properties of polycarbonate layered-silicate nanocomposites. Polym Eng Sci 2004;44:825–34.
[7] Qin H, Zhang S, Liu H, Xie S, Yang M, Shen D. Photo-oxidative degradation of polypropylene/montmorillonite nanocomposites. Polymer 2005;46:3149–56.
[8] Mani G, Fan Q, Ugbolue SC, Yang Y. Morphological studies of polypropylene-nanoclay composites. J Appl Polym Sci 2005;97:218–26.
[9] Langat J, Bellayer S, Hudrlik P, Hudrlik A, Maupin PH, Gilman JW, et al. Synthesis of imidazolium salts and their application in epoxy montmorillonite nanocomposites. Polymer 2006;47:6698–709.
[10] Calcagno CIW, Mariani CM, Teixeira SR, Mauler RS. The effect of organic modifier of the clay on morphology and crystallization properties of PET nanocomposites. Polymer 2007;48:074–966.
[11] Dennis HR, Hunter DL, Chang D, Kim S, White JL, Cho JW, et al. Effect of melt processing conditions on the extent of exfoliation in organoclay-based nanocomposites. Polymer 2001;42:9513–22.
[12] Severe G, Hsieh AJ, Koene BE. Effect of layered silicates on thermal characteristics of polycarbonate nanocomposites ANTEC 2000. Society of Plastics Engineers Technical Papers. Conference Proceedings, vols. I–III: 2000. p. 1523–6.
[13] Srinath G, Gnanamoorthy R. Effect of nanoclay reinforcement on tensile and tribo behaviour of nylon 6. J. Mater Sci 2005;40:2897–901.
[14] Jia QM, Zheng M, Xu CZ, Chen HX. The mechanical properties and tribological behavior of epoxy resin composites modified by different shape nanofillers. Polym Adv Technol 2006;17:168–73.
[15] Jawahar P, Gnanamoorthy R, Balasubramanian M. Tribological behaviour of clay-thermoset polyester nanocomposites. Wear 2006;261:835–40.
[16] Jawahar P, Gnanamoorthy R, Balasubramanian M. Flexural and tribological properties of polyester-clay nanocomposites. J Mater Sci 2005;40:4391–3.
[17] Lai SQ, Li TS, Liu XJ, Lu RG, Yue L. The tribological properties of PTFE filled with thermally treated nano-attapulgite. Tribol Int 2006;39:541–7.
[18] Lai SQ, Li TS, Liu XJ, Lu RG. A study on the friction and wear behavior of PTFE filled with acid treated nano-attapulgite. Macromol Mater Eng 2004;289:916–22.
[19] Arias CB, Zaman AA, Talton J. Rheological behavior and wear abrasion resistance of polyethylene oxide/laponite nanocomposites. J Disper Sci Tech 2007;28:247–54.
[20] Xiang DH, Gu CJ. A study on the friction and wear behaviour of PTFE filled with ultra-fine kaolin particulates. Mater Lett 2006;60:689–92.
[21] Dasari A, Yu ZZ, Mai YW, Hu GH, Varlet JH. Clay exfoliation and organic coating modification on wear of nylon 6 nanocomposites processed by different routes. Compos Sci Technol 2005;65:2314–28.
[22] Carrión FJ, Sanes J, Bermúdez MD. Influence of ZnO nanoparticle filler on the properties and wear resistance of polycarbonate. Wear 2007;262:1504–10.
[23] Carrión FJ, Sanes J, Bermúdez MD. Effect of ionic liquid on the structure and tribological properties of polycarbonate-zinc oxide nanodispersions. Mater Lett 2007;61:4531–5.
[24] Lloyd DJ, In: Hansen N, Juuljensen D, Leffers T (Eds.). Proceedings of the twelfth Risø international symposium on materials science: 1991. p. 81–99.
[25] Scalon JD, Fieller NRJ, Stillman EC, Atkinson HV. Spatial pattern analysis of second phase particles in composite materials. Mater Sci Eng A 2003;356:245–57.
[26] Morisita M. Memoirs of the faculty of science, Kyushu University, Series E. Biology 1959;2:215–35.
[27] Ohser J, Mücklich F. Statistical analysis of microstructures in materials science. Chichester: John Wiley & Sons; 2000.
[28] Li XG, Huang MR. Thermal degradation of bisphenol A polycarbonate by high-resolution thermogravimetry. Polym Int 1999;48:387–91.
[29] Standard Practice for Plastics: Dynamic Mechanical Properties: Determination and Report of Procedures. ASTM D4065, 2001.
[30] Valera-Zaragoza M, Ramírez-Vargas E, Medellín-Rodríguez FJ, Huerta-Martínez BM. Thermal stability and flammability properties of heterophasic PP–EP/EVA/organoclay nanocomposites. Polym Degrad Stab 2006;91:1319–25.